THE ASTROPHYSICAL JOURNAL, 539:124–135, 2000 August 10

RESOLVING THE JEANS MASS IN HYDRODYNAMIC SIMULATIONS OF HIERARCHICAL CLUSTERING

ERIC R. TITTLEY[1] AND H. M. P. COUCHMAN[2]
Department of Physics and Astronomy, University of Western Ontario, London, Ontario N6A 3K7, Canada;
tittley@umbc.edu, couchman@physics.mcmaster.ca
Received 2000 January 3; accepted 2000 March 2

ABSTRACT

We examine the necessity of resolving the Jeans mass in hydrodynamical simulations of the hierarchical formation of cosmological structures. We consider a standard two-component fluid and use smoothed particle hydrodynamics to model the baryonic component. It is found that resolution of the Jeans mass is not necessary to extract bulk properties of bound objects that are independent of resolution, provided that the objects have undergone a number of merger events. The degree of merging must be sufficient to populate the objects with substructure of similar total mass. After this criterion is met, neither the density profiles of structures nor their density-temperature distributions depend appreciably on the resolution of the simulation. Resolution of the Jeans mass by the imposition of a minimum temperature is not found to affect adversely the state of the matter in the final clusters. The baryon concentration profiles still indicate a deficit of gas with respect to the dark matter in the interiors of the dense halo structures. This is offset by a baryon enrichment in the filamentary and sheetlike structures as well as the voids.

Subject headings: galaxies: clusters: general — hydrodynamics — large-scale structure of universe — methods: numerical

1. INTRODUCTION

Numerical simulations have proved useful for understanding the history and dynamics of cosmological structure (Davis et al. 1992; Katz 1992; Cen et al. 1994; Evrard, Metzler, & Navarro 1996). Our ability to model collisionless systems has matured to the extent that bulk properties of the dark matter can be predicted with increasing confidence, although important exceptions exist, such as the merger rates of substructure as well as the inner profiles of dark matter halos (see, for example, Moore et al. 1998).

Combining collisionless N-body techniques with a hydrodynamical method to follow the baryonic component opens the way to a detailed understanding of cosmic structure formation in a variety of models. Modeling the baryonic component removes the need to make assumptions about the relationship between the baryonic material and the underlying collisionless matter. Such techniques have proved to be both popular and powerful (Hernquist & Katz 1989; Evrard 1990; Katz & Gunn 1991; Cen 1992; Navarro & White 1993; Steinmetz & Müller 1993; Ryu et al. 1993; Bryan et al. 1994; Gnedin 1995; Steinmetz 1996). An early review of hydrodynamic codes (Kang et al. 1994b) indicated that global averages of physical quantities did generally converge among the codes with increasing resolution, though errors in mean density and mean temperature varied by up to 20%. A more recent comparison of several hydrodynamic codes (Frenk et al. 1999) has shown that we may begin to have confidence in the overall properties of the baryonic distribution predicted by these codes. However, several differences which are apparent both between codes and between results of varying resolution suggest that convergence has yet to be established conclusively. We address here the particular issue of convergence with resolution in hydrodynamic simulations in which objects are built up through hierarchical merging. We do not consider radiative cooling in this work.

In the standard model of cosmological structure formation, larger structures are formed via the amalgamation of smaller structures formed at earlier times in a hierarchical fashion. In any simulation which models the formation of such structures in this hierarchical manner, there will be an abundance of objects formed at the resolution limit of the simulation. Numerical effects will be a particular problem for these objects. The propagation of these effects into the larger objects subsequently formed requires characterization both to determine the reliability of the physical model and to ensure convergence among simulations performed at various resolutions.

Recently Owen & Villumsen (1997) have argued that it is necessary to resolve the Jeans mass in a simulation if convergence is to be attained with increasing resolution. This requires that a minimum temperature be imposed in the simulation such that the gas in the first bound objects—which form at the resolution limit in a standard simulation of hierarchical clustering—is at a sufficient temperature to support itself via pressure in the gravitational potential well of the first dark matter structures. The authors argue that if the gas temperature is initially much less than the virial temperature of the first halos (this is a boundary condition frequently adopted in cosmological simulations), the cold gas falling into the first potential wells will suffer spuriously large amounts of shock heating of the gas. This "shocking" will be greater for simulations with lower resolution, since the scale over which the shocks occur will be larger. Conversely, if the initial generation of objects is pressure-supported, the interaction of the baryons in merging halos as the hierarchical structure formation proceeds will lead only to weak shocks. (This result follows since the velocity with which lumps merge is similar to the internal velocity dispersion of the individual lumps in a typical hierarchy.)

[1] Present address: Department of Physics, University of Maryland, Baltimore, MD 21250.
[2] Present address: Department of Physics and Astronomy, McMaster University, Hamilton, Ontario L8S 4M1, Canada

Owen & Villumsen (1997) suggest that the difference in the amount of shock heating at early stages will persist through to the final object and prevent convergence of numerical results unless a minimum temperature is imposed.

Owen & Villumsen (1997) find, in scale-independent simulations, that without the imposition of a minimum temperature to pressure-support resolution-limited structures, the gas is found to move en masse toward a state of higher density and lower temperature as the resolution of the simulation increases. This behavior is not to be expected during the formation of hydrostatic structures. In the standard model, we expect the virial temperature of a structure to be broadly determined by its mass, following the relationship $T \propto M^{2/3}$. Since the bulk of the gas resides in the halos of these structures, the temperature of the bulk of the gas should consequently be determined by the dark matter distribution, a distribution whose convergence among differing resolutions is confirmed in the simulations of Owen & Villumsen (1997).

There are other issues of concern raised by the results of the simulations described in Owen & Villumsen (1997). First, the results suggest paradoxically that the injection of thermal energy into a system at an early time can lead to a cooler system at a later time. The authors claim that this is achieved by reducing the amount of shock heating as the first, unresolved, objects collapse. However, the injection of thermal energy into the system via the imposition of a minimum temperature preheats the gas in a manner which is essentially equivalent to shock-heating the gas in the first objects.

Another concern is the concentration of baryons relative to the dark matter in the cores of structures reported in Owen & Villumsen (1997). In three-dimensional simulations without cooling, spanning a wide range of resolutions, others have found *extended* distributions of baryonic material, relative to the dark matter (Evrard 1990; Thomas & Couchman 1992; Cen & Ostriker 1993; Kang et al. 1994a; Metzler & Evrard 1994; Pearce, Thomas, & Couchman 1994; Navarro, Frenk, & White 1995; Anninos & Norman 1996; Lubin et al. 1996; Pildis, Evrard, & Bergman 1996). Pearce et al. (1994) explains the phenomenon as a result of the merging process in which gas is shocked, permanently removing energy from the dark matter component and passing it to the gas.

A possible explanation for the conflicting results regarding the baryon concentration may be that the simulations of Owen & Villumsen (1997) were done using a two-dimensional code. This allowed them to achieve high spatial resolutions but may have introduced phenomena unique to two-dimensional geometries.

1.1. *Jeans Mass in a Two-Component Fluid*

In a self-gravitating baryonic fluid, the Jeans mass is easily obtained, by a perturbatitive analysis, as a sharp threshold between acoustic oscillation and collapse, depending on the density and temperature of the fluid. In a two-component fluid comprised of baryons and collisionless cold dark matter, the situation is more complicated. The low initial velocity dispersion of cold dark matter leads to instability, or growth, in this component on all scales. The relevant question in this case for the baryonic fluid is on what scales do the two components remain coupled adiabatically? On small scales, gas pressure will be sufficient to oppose the gas falling into the small dark matter potential wells, whereas on large scales the initial gas temperature will be lower than the effective virial temperature of the forming dark matter halo and the gas will increase in overdensity with the dark matter. A perturbative analysis of the coupled two-component fluid is relatively straightforward but not very illuminating for our purposes. In particular it can be shown that there is not a single Jeans mass in the sense described above (see Peacock 1999, for example). It is sufficient for our purposes to define the Jeans mass as that which is just sufficient to adiabatically compress the gas to an overdensity which is the same as that of the dark matter.

With this assumption we can approximate the Jeans mass of the gas for a fluid composed of collisionless dark matter of density $\rho_{\rm DM}$ and collisional baryonic material (gas) of density ρ_g and temperature T by

$$M_{\rm J} \simeq \frac{\rho_g}{2}\left(\frac{1}{{\rm G}\rho_M}\frac{kT}{\mu m_{\rm H}}\right)^{3/2}, \qquad (1)$$

where the total mass density is given by $\rho_M = \rho_{\rm DM} + \rho_g$.

1.2. *The Minimum Temperature for Pressure Support*

The effective mass resolution of a simulation is usually fixed. For simulations such as those described here which use smoothed particle hydrodynamics (SPH) to model the gas forces, this can be taken to be the total mass of the number of particles, $N_{\rm SPH}$, over which local quantities are averaged, presuming all gas particles have equal mass. The number of particles is typically of the order of 30. Associating the mass of this number of particles to the Jeans mass (eq. [1]) and assuming a total mass density, ρ_M in equation (1), equal to the mean density of the simulation volume, $\overline{\rho}_M$, the temperature required to support gas in dark matter halos of this size is

$$T_{\rm min} = \left(\frac{2N_{\rm SPH}m_g}{\overline{\rho}_g}\right)^{2/3} G\overline{\rho}_M \frac{\mu m_{\rm H}}{\rm k}, \qquad (2)$$

where m_g is the mass per gas particle. For a flat universe with the mean gas density related to the mean mass density by $\overline{\rho}_g = \overline{\rho}_M \Omega_g/\Omega_M$, equation (2) may be expressed in a form more appropriate for cosmological simulations. Noting that the mean matter density scales with the expansion factor, a, as $\overline{\rho}_M = \overline{\rho}_M^f (a_f/a)^3$, with a_f the expansion factor at the present and $\overline{\rho}_M^f$ equal to the critical density ρ_c, we get

$$\frac{T_{\rm min}}{\rm K} = 1.6 \times 10^4 \left(hN_{\rm SPH}\frac{m_g}{10^{10}\,M_\odot}\frac{\Omega_M}{\Omega_g}\right)^{2/3}\frac{a_f}{a}. \qquad (3)$$

If the gas has a minimum temperature set by this value, then it can be assumed that the simulation is resolving the Jeans mass. This assumption is flawed in a number of ways. Since local density is not in general equal to the mean in the simulation, the minimum temperature should also be a function of position. However, the minimum temperature should vary with the local density as $T_{\rm min} \simeq \rho_M^{1/3}$, which is not a particularly sensitive function, especially in those regions in which the first objects are forming. More significant is the decoupling of the components of the fluid, discussed previously. This is likely to occur for the first objects formed since the dark matter halos collapse regardless of whether or not the gas is pressure-supported. For those situations in which, locally, $\rho_{\rm DM} \gg \rho_g$, enhancement of the dark matter density without a similar increase in the gas

density requires the temperature to rise by an equivalent fraction in order to maintain a constant Jeans mass for the gas. However, during the formation of these dark matter structures, the gas will be allowed to gradually respond, adiabatically, to the increasing gravitational potential, partially or fully offsetting the need for an increased minimum temperature. This would not occur without the initial minimum temperature, since the gas in that case would initially collapse along with the dark matter.

The simulations of Owen & Villumsen (1997) impose a minimum temperature that is constant in time. This permits a physical justification for the minimum temperature in the form of reheating of the intercluster medium due to the first epoch of star formation. However, it has two serious drawbacks. First, it breaks the scale invariance of their results. A fixed minimum temperature will be equal to the appropriate minimum temperature required to pressure-support resolution-limited structures only at one epoch. This epoch will change, depending on the scale of the simulation. Second, it undermines Owen & Villumsen's conclusion that pressure support for the first objects formed is required to achieve convergence, since their first objects are, in fact, not pressure-supported.

1.3. *The Hypothesis*

In this paper, we propose that the effect on the state of the gas of poorly resolving the first baryonic structures does not propagate into larger structures formed through hierarchical merger. The properties of the gas in the larger halos will be determined primarily by the virial properties of the structures that are dominated by the distribution of the collisionless component.

To test this hypothesis, we performed a series of seven simulations of hierarchical structure formation. The simulations were done at three different resolutions. For two of these simulations, the temperature of the gas content was prevented from being less than the temperature required to maintain pressure support for the smallest resolvable object; that is, the Jeans mass was resolved.

Comparison of the data simulated for this study was made using both the total sample of gas in each simulation volume as well as an individual well-resolved structure. Using an individual cluster permits examination of those effects that are frequently the focus of interest in structure formation simulations; the void particles in simulations of this sort are usually ignored because of a lack of resolution in this regime.

We examine the entropy of the gas, which is a measure of the degree of shocking. Also examined is the density distribution of the gas to determine the extent of any bulk movements of the gas to higher densities as resolution is increased. We also explore mean bulk properties of the structures: in particular, the mean dark matter and gas density profiles and the mean baryon fraction profile. The mean gas density and baryon fraction profiles are potentially sensitive to a lack of convergence as well as being of fundamental interest.

The outline of the paper is as follows. The simulations are described in § 2. The results of an attempt to re-create the results of Owen & Villumsen (1997), but using a three-dimensional geometry, are given in § 3.1. The impact of resolving the Jeans mass on the final state of the gas in galaxy clusters is addressed in § 3.2. A look at the variation in the normalized baryon fraction distribution is taken in § 3.3. The results are discussed in § 4. Hereafter we refer to Owen & Villumsen (1997) as OV97.

Although the simulations are scale-invariant, the results on occasion are given in physical units. This is simply a matter of convenience for the purpose of comparison.

2. THE SIMULATIONS

The N-body code with SPH, HYDRA (Couchman, Thomas, & Pearce 1995), was used for all simulations. HYDRA calculates the gravitational forces using an adaptive mesh for the large-scale complemented with particle-particle calculations for the short-range forces. SPH is used for the hydrodynamics.

Seven simulations were performed. Five used the original code, and two used a variant of HYDRA that imposes a minimum temperature on the gas particles. The details of the simulations are outlined in Table 1. Given there are the number of particles of each type and the gravitational softening length, ϵ. The simulations that were evolved to the final expansion factor, $a = a_f$, were performed twice, once with and once without a minimum temperature, whereas the first trio were evolved only once, without a minimum temperature. Initial density perturbations are the same for all resolutions within a group, albeit limited by the Nyquist frequency.

The minimum temperature is set to support a mass of particles corresponding to the effective mass resolution of the simulation as described in the Introduction. At each epoch of the simulation, structures composed of $N_{\rm SPH}$ gas particles with a local density equal to the mean gas density

TABLE 1

SIMULATION PROPERTIES

	Number of Particles		
Resolution (1)	Gas (2)	Dark Matter (3)	ϵ (h^{-1} kpc) (4)
Evolved to $a = 0.17a_f$			
32^3	32^3	32^3	80
64^3	64^3	64^3	40
128^3	128^3	128^3	20
Evolved to $a = 0.22a_f$ and a_f			
32^3	32^3	32^3	80
64^3	64^3	64^3	40

of the volume, $\overline{\rho}_g$, and individual masses of m_g are supported against collapse by the imposition of a minimum temperature, $T_{\min}$. The minimum temperature is derived by simply equating the Jeans mass, M_J, to the structure mass $N_{\rm SPH} m_g$, as is done in § 1.2 to derive equation (2).

During the two simulations in which a minimum temperature was imposed, $T_{\min}$ was recalculated at each epoch. Since the minimum temperature scales with the mean density as $T_{\min} \propto \overline{\rho}^{1/3}$, then it scales with the expansion factor, a, as $T_{\min} \propto a^{-1}$. Normally, adiabatic cooling for a uniform monotonic gas would maintain the relation $T \propto a^{-2}$. Consequently, the imposition of the minimum temperature has the effect of continuously injecting thermal energy into the fraction of the gas whose adiabatic expansion would bring its temperature below the minimum temperature.

Although the simulations are scale-invariant, it may be useful to give numbers to the actual minimum temperatures used in the simulations. The number of particles per mass resolution was $N_{\rm SPH} = 52$. This leads to mass resolutions of 4.3×10^{12} and $5.4 \times 10^{11}\ M_\odot$ for the 32^3 and 64^3 simulations, respectively. The physical scale of these simulations is described in more detail below. For those simulations in which a minimum temperature is imposed, the values of $T_{\min} = (3.0 \times 10^6\ {\rm K}) a_f/a$ and $(7.5 \times 10^5\ {\rm K}) a_f/a$ for the 32^3 and 64^3 simulations, respectively, were consequently used. For comparison, the simulations of OV97 used fixed minimum temperatures of either 2.1×10^6 or 3.4×10^7 K (Owen & Villumsen 1996). The temperature of the halo gas in a virialized system goes roughly as $T = 7 \times 10^7 [M/(10^{15}\ M_\odot)]^{2/3}$ K (Tittley & Couchman 1999). This gives virial temperatures of 8.6×10^6 and 2.2×10^6 K for objects formed at the resolution limit in the 32^3 and 64^3 simulations, respectively, presuming no change in the baryon fraction. The imposed minimum temperatures are then about one-third of the virial temperatures of the structures that would form at the resolution limit.

The initial conditions for the two-dimensional simulations of OV97 have a density perturbation spectrum with a spectral index equivalent to the three-dimensional $n = -1$ form used in the simulations presented here. Because the simulations are scale-free, the spatial variance of the density fluctuations at the end of the simulation in the larger volume corresponds to an earlier epoch in the smaller volume, after scaling by the box size.

The amplitude of linear density fluctuations, as measured by the power spectrum of the density field, $P(k)$, relates to the wavenumber of the fluctuation, k, measured in comoving coordinates, and the time, t, via

$$P(k) \propto \left(\frac{\sigma_L}{h}\right)^2 k^n t^{4/3}\ , \tag{4}$$

where σ_L is a normalization factor corresponding to the assumed value of the variance, σ, of the present density field on the scale of L.

Although the simulations discussed in OV97 and those presented here are scale-invariant, it is useful to set a physical size to the simulation volume. Indeed, this may be a benefit to those readers familiar with the scale of cosmological structures. Further, this is the only practical way we have of determining the degree of clustering in the simulations of OV97. OV97 uses a volume with a side of length $128\ h^{-1}$ Mpc, $h = 0.5$ (Owen & Villumsen 1996). Since we use a volume with sides $40\ h^{-1}$ Mpc and $h = 0.65$, this gives a ratio of scales of 4.16 for their simulation scale compared to the simulations described here. For the normalization factor, they have $\sigma_8 = 0.6$, whereas we used $\sigma_8 = 0.935$. This implies an expansion factor of $0.24 a_f$. That is, the structures in the simulations presented here, scaled by the box size, will have grown in similar magnitude to those of OV97 after an expansion of 0.24 of the final expansion factor of the simulation.

In this study, the data have been compared at the slightly earlier expansion factors of $0.17 a_f$ and $0.22 a_f$ to ensure that structures have not undergone more than a couple of merger events. As a check, a volume with the same cosmological parameters as described in OV97 but with the same perturbation waves as found in our smaller boxes was evolved to an expansion factor a_f. The data from the $40\ h^{-1}$ Mpc volumes at an expansion factor of $0.22 a_f$ are visibly similar to the final output of this test volume, supporting the legitimacy of scaling the numerical results.

It was feasible, computationally, to evolve the volume to the present only at the resolutions of 2×64^3 particles and less. Hence, this study will concentrate on a comparison of the simulations of resolution corresponding to this number of particles with simulations of a resolution appropriate to 2×32^3 particles. These resolutions will be referred to henceforth as the 64^3 and 32^3 simulations. Each was evolved with and without a minimum temperature. For the earlier epoch corresponding to the expansion factor of $0.17 a_f$, the volume could also be evolved at the resolution provided by 2×128^3 particles. Thus a set of three simulations was performed using the same density perturbations (limited by the Nyquist frequency) at resolutions corresponding to 128^3, 64^3, and 32^3.

Cooling was neglected to maintain the scale invariance. In all simulations, $\Omega = 1$, $\Omega_{\rm DM} = 0.9$, and $\Omega_g = 0.1$.

The initial density perturbations were established by displacing the particle positions from a uniform cubic grid using the Zeldovich (1970) approximation for growth of density perturbations in the linear regime in the standard way.

The initial redshift for the 32^3 and 64^3 simulations is $z_{\rm init} = 75$. This was chosen to keep the maximum displacement incurred during the establishment of the density field to less than half the initial grid spacing. This ensures that the correct nonlinear field will be attained at later times. The same criterion was used to set the initial redshift for the 128^3 simulation for which $z_{\rm init} = 150$.

3. RESULTS

3.1. *The State of the Baryons at an Early Epoch*

We first attempt to reproduce the results of OV97 by examining the state of the baryons in our simulations at an epoch comparable to that of the final epoch of the simulations of OV97. The smaller physical scale of the simulations presented here requires that we examine our data before the nominal end of the simulation in order that a comparable level of clustering has developed to that present at the final epoch of the simulations of OV97. The required expansion factor is $a = 0.22 a_f$, where a_f is the final expansion factor of the simulations.

Following the analysis given by OV97, we look at the distribution of the gas particles in the ρ-T plane as well as the density distributions for which the density is resampled

down to the resolution of the lowest resolution runs as described below. The position within the ρ-T planes gives an indication of the degree of shocking, with the more highly shocked gas (gas with greater entropy as indicated by $T\rho^{-\gamma}$, $\gamma = \frac{2}{3}$) lying to the upper left (high temperature, low density).

In order to allow a direct comparison of the densities in simulations of different resolution, a density resampling technique was employed. The (resolution-degrading) resampling was accomplished by smoothing over equal masses for each particle using an SPH-like density estimate. Consequently, there are approximately 8 times as many particles in each estimate for the 64^3 data as in the 32^3 data, but the smoothing radii are approximately the same. This resolution degradation is performed for the high-resolution simulations (64^3) when comparison is made with the lowest resolution simulation (32^3). This technique was unfortunately not possible with the 128^3 data set, owing to the computational effort of summing over the more than 3000 neighbor particles of each gas particle. In this case, resolution degradation was performed by sampling 32^3 particles randomly from the set of 128^3, increasing the mass of each particle appropriately, and recalculating the smoothing lengths and densities. Although computationally more efficient, this method has the drawback of introducing extra shot noise. This is the method used in OV97.

It is clear that for density profiles without cores, higher mass and spatial resolutions will lead to more gas at a higher density even if the simulations can be said to have converged to the true solution within resolution limits. If the densities are averaged within volumes encompassing a mass which is resolved in the lowest resolution simulation, then these masses should not vary significantly.

The simulations of OV97 produce more cool, dense gas as the resolution increases. OV97 interpret this to mean that in the higher resolution simulations, the gas in the cores of structures is not as strongly shocked. To search for this effect, three sets of data were evolved at the resolutions provided by 2×32^3, 2×64^3, and 2×128^3 particles, half in each phase of gas and dark matter, as described in § 2. Each set has the same initial perturbations, limited appropriately in the high spatial frequency domain by the Nyquist frequency. These data sets were evolved to an early epoch for which the amplitude of density fluctuations has grown to a level comparable to those in the data presented by OV97.

The evolved data were resampled, in the case of the 64^3 and 128^3 sets, to the same mass resolution as the 32^3 set using the same method used in OV97, which involves randomly selecting 32^3 particles from each phase. This avoids the problem of performing the density estimate over the very large number of neighbor particles required for the 128^3 data set, at the expense of an increase in shot noise. Local SPH density estimates for the sampled particles in these resampled sets were determined allowing comparisons of the data in ρ-T space.

The ρ-T distributions for all the gas in each of these three simulations are illustrated in Figure 1 (*top panels*). This is comparable to the top panels of Figure 8 of OV97. It is clear that there is no trend for the *bulk of the mass* to move toward a cooler and denser state as the resolution increases, in contrast to the results of OV97. Since the bulk of this gas is in the halos of bound structures, the argument given in the Introduction is supported; the entropy of the gas is set by the virial properties of the halo which are dictated by the dark matter. There is a trend for the void particles (found to the lower left in the ρ-T plane) to increase in temperature as the resolution increases. There is also a trend for the distributions to become more diffuse, particularly toward the denser and cooler state.

The lower set of panels in Figure 1 give the distribution for particles in a cluster common to all three sets of data. The cluster was selected simply for being one of the larger clusters of particles to have formed by this early stage. The cluster is barely resolved (~ 100 particles) in the 32^3 simulation but is well resolved in the 128^3 simulation. Here it is evident that the diffusion of the distributions to a denser and cooler state is due to a small population of particles, and not a bulk movement. Upon examination of the spatial distribution of this population, these particles are found to be located in substructure that is present only in the simulations with greater mass resolution. These clumps are not as shocked as the particles in the halos of the substructure. This is consistent with the phenomenon described by OV97 in nature, though not in extent since it is not a bulk motion but simply a new population of particles.

As the mass resolution increases, the first bound halos form at earlier epochs at higher densities leading to increased central densities in the final dark matter halos. This is illustrated in Figure 2, which compares the gas and dark matter mean density profiles for resolved clusters in the simulations, albeit at a later epoch. The dark matter density is double in the 64^3 simulation compared with the 32^3 simulation in the central regions (close to the resolution limit of the 32^3 simulation). This *increases* the degree of shocking of the halo particles more than offsetting the decreased amount of shocking in the cores of substructure. The mean temperature of this structure thus *increases* with increasing resolution: in physical units it is 2.9×10^7, 3.2×10^7, and 4.5×10^7 K for the 32^3, 64^3, and 128^3 simulations, respectively. The total amount of shocking on the whole also increases, but not to such a degree. The amount of shocking, as measured by the mass-weighted mean of the entropy parameter, $\langle T/\rho_g^{2/3}\rangle_M$, for an individual cluster at the three resolutions evolved to $a = 0.17a_f$, is given in Table 2. The values not resolution-degraded are given in column (2), which reveals a slight increase (10% for every doubling in resolution) in the entropy as the resolution increases. If the densities are recalculated for the resampled data with the intent of comparing similar effective resolutions, then the degree of shocking decreases quite markedly with increasing resolution (Table 2, col. [3]). This occurs simply because the temperatures of the particles are not changing while the resampled densities of the particles in the densest regions decrease as a result of the use of a larger smoothing radius. It would be erroneous to conclude that the gas is actually less shocked, since the temperature

TABLE 2

MEASURE OF SHOCKING OF AN INDIVIDUAL CLUSTER

	$\langle T/\rho_g^{2/3}\rangle_M$ (K cm^2 g$^{-2/3}$)	
RESOLUTION (1)	Unsampled (2)	Sampled and Recalculated ρ_g (3)
32^3	5.5×10^{24}	5.5×10^{24}
64^3	5.9×10^{24}	1.6×10^{24}
128^3	6.5×10^{24}	0.5×10^{24}

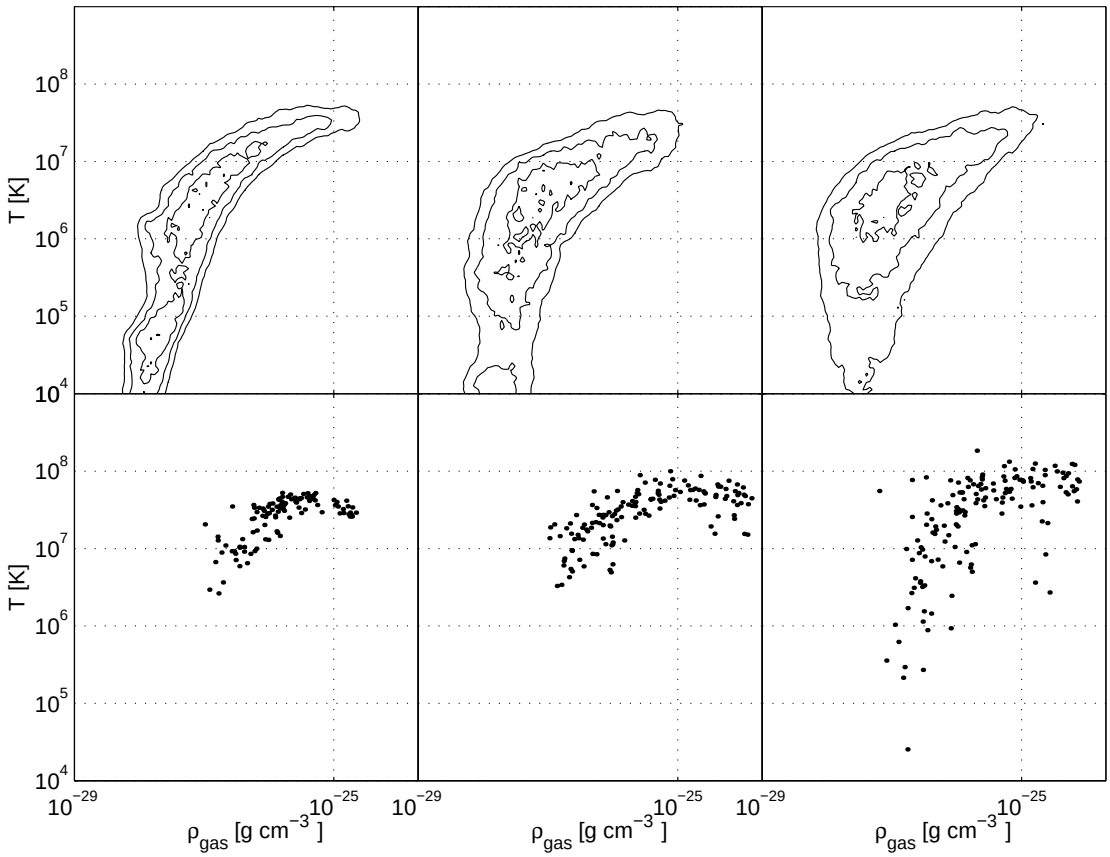

FIG. 1.—Temperature vs. gas density at a timescale factor $a = 0.17a_f$. The upper set of panels are for all the gas, while the lower set is for a selected cluster. From left to right, the panels correspond to simulations with increasing resolutions of 32^3, 64^3, and 128^3 baryon particles. The simulation data were resampled before analysis to the same mass resolution as the 32^3 simulation. Contour lines in the upper panels are of constant mass surface density in ρ-T space. In the lower set of panels, the data points are for the sample of particles in the selected cluster.

of the halo gas particles and the depth of the potential well are so intimately related.

The gas density distributions for both the 32^3 and 64^3 data were found at an expansion factor of $0.22a_f$. The densities of the 64^3 data set were resampled as described previously. The distribution of gas density at this early epoch (Fig. 3, *left-hand panels*, *dashed lines*) is only weakly dependent on resolution, becoming somewhat less peaked at

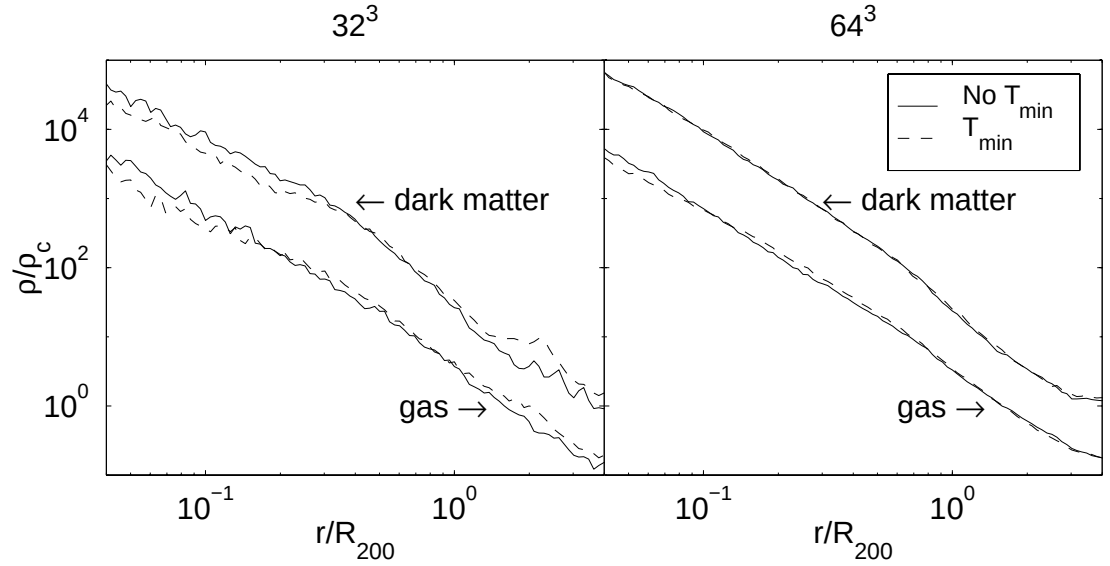

FIG. 2.—Mean dark matter and gas density profiles. The panel to the left corresponds to the low-resolution set of runs, while the panel on the right is for the high-resolution set. Profiles are given for clusters formed in the absence of a minimum temperature and for clusters formed in a simulation with a minimum temperature scaled appropriately for the mean gas density at each epoch.

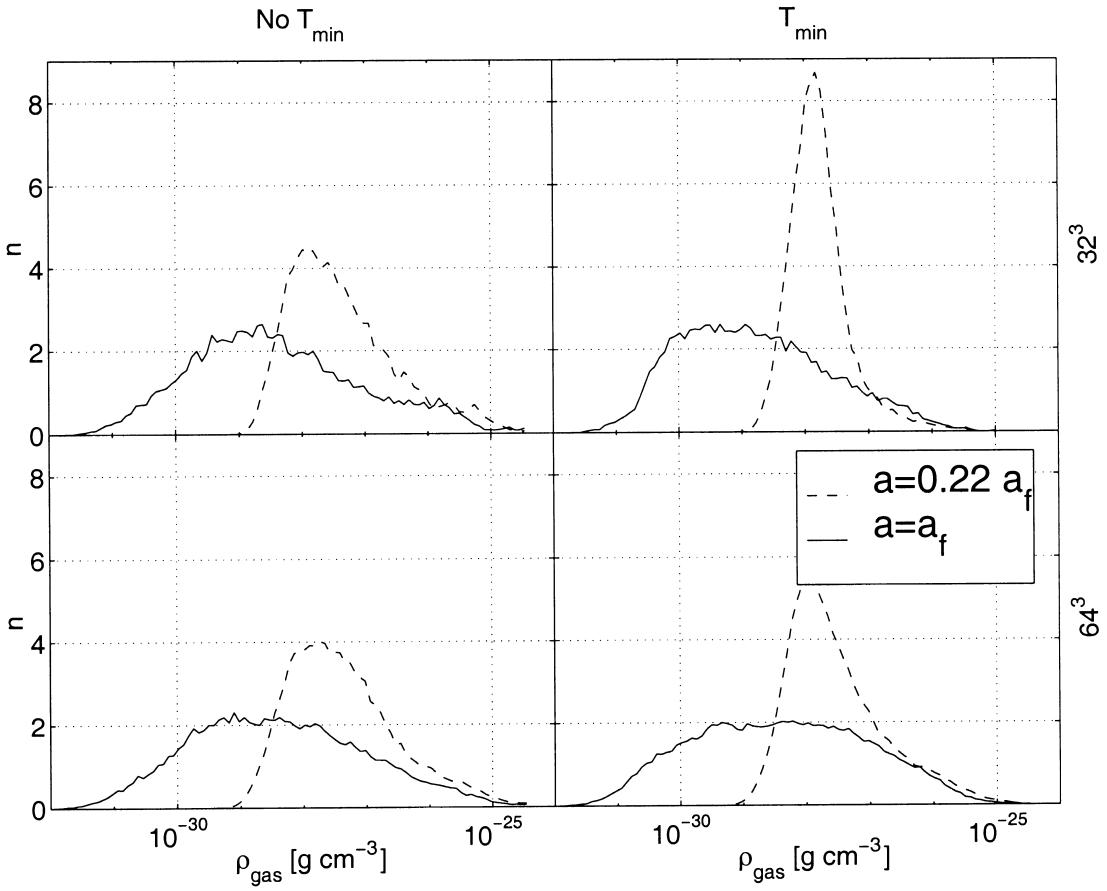

FIG. 3.—Distribution of gas density at early and late epochs. The upper set of panels is for the 32^3 set of data, while the lower set is for the 64^3 set. From left to right, the panels correspond to no minimum temperature and a minimum temperature scaled appropriately for the epoch.

10^{-28} g cm^{-3} at the higher resolutions. No bulk motion of the gas to higher densities is observed, in contrast to the simulations described in OV97.

Since no bulk motion of the gas to higher densities and lower degrees of shocking is observed, we might predict that the imposition of a minimum temperature will not significantly affect these results. The distribution of the gas within the ρ-T plane at the early epoch of $a = 0.22a_f$ is illustrated in Figure 4. Again, the bulk of the gas is found in the same state in both simulations without a minimum temperature (Fig. 4, *left-hand panels*), with a diffusion toward a state of lower entropy. For those simulations in which a minimum temperature is imposed (Fig. 4, *right-hand panels*), the gas is displaced within the ρ-T plane in those regions below $T_{\rm min}$ (for obvious reasons) and below the locus that uniform gas would trace if it were allowed to cool to the minimum temperature appropriate at each epoch. In order for gas to be found below this locus, it must be initially held at a high temperature and density but with little or no increase in entropy and subsequently allowed to cool adiabatically. The bulk of the gas is above these boundaries. The gas that is above these boundaries is consistently located in similar proportions to the gas found in the same locations in the ρ-T plane in the simulations without a minimum temperature. There is no gas in the lower resolution simulations that fits these criteria, however.

The resampled density distributions for the simulations with a minimum temperature, illustrated in Figure 3 (*right-hand panels, dashed lines*), confirm that the minimum temperature does modify the distributions but does not provide convergence. This figure is comparable to Figure 6*d* in OV97, which indicates a bulk motion to higher densities as the resolution is increased, even when the data are resampled to the scale of the lowest resolution simulation. In our simulations, for the gas denser than 10^{-27} g cm^{-3}, there is actually a decrease in the agreement between the lower and higher resolution data when a minimum temperature is enforced.

The decrease in the degree of shocking reported by OV97 as the resolution of a hydrodynamic simulation is increased is confirmed in the cores of clusters of particles. However, the bulk movement of the gas particles to a less shocked state is *not* observed in our simulations. Indeed, the mean degree of shocking of cluster particles is essentially conserved, with the mean temperature of particles actually increasing with resolution. The displacement in density distributions reported by OV97 is also not observed, nor is any sort of convergence provided by the imposition of a minimum temperature.

3.2. *The State of the Baryons at a Late Epoch*

After many mergers, it is possible that the gas in the initial structures described above will have "forgotten" the degree of shocking it had at early times. It may have been sufficiently shocked by subsequent mergers that early heating, via strong shocks or otherwise, would no longer be significant to the total thermal content and distribution. To examine this hypothesis, the 32^3 and 64^3 sets of simulations

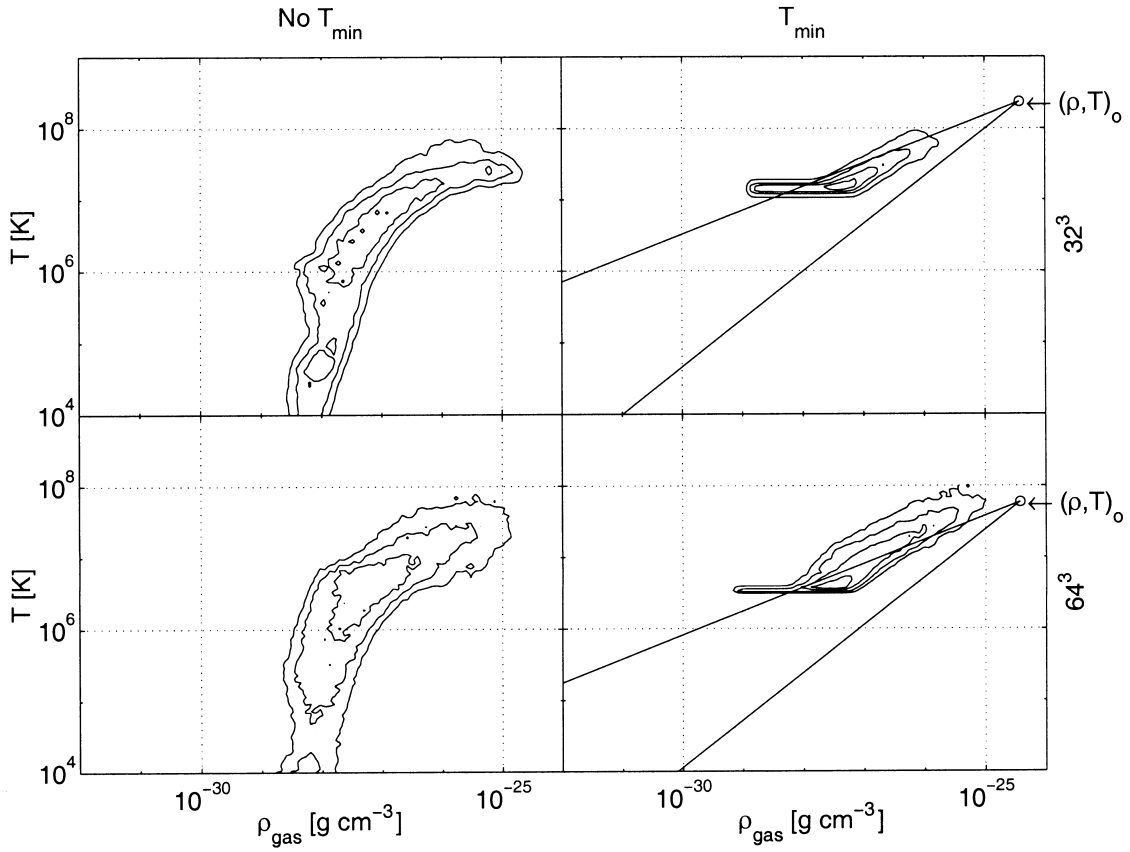

FIG. 4.—Temperature vs. gas density for all the gas at an expansion factor of $a = 0.22a_f$. The circles in the right-hand panels indicate the starting density and temperature. For the left-hand panels, these points are off the figure at $T = 100$ K. The lines projecting to the lower left of each circle correspond to the path taken by a uniform gas expanding and cooling adiabatically (*lower line*) and to the path of gas maintaining $T_{\min}$ (*upper line*). The panels are arranged as in Fig. 3.

used in § 3.1 were evolved to a further state which involved many levels of merging. It is not presently feasible to evolve a 128^3 to such a state with the hardware on hand in a manageable amount of time.

The gas distributions in the ρ-T plane at this end state are illustrated in Figure 5. At densities less than $\sim 5 \times 10^{-26}$ g cm^{-3}, the distributions for the 32^3 (*top left*) and 64^3 (*bottom left*) simulations are identical in form. At $\sim 5 \times 10^{-26}$ g cm^{-3}, it is the lower mass resolution simulation that produces the greatest amount of cool, dense gas.

Evolving these sets of data while enforcing a minimum temperature sufficient to pressure-support structures with $N_{\rm SPH}$ or fewer particles does little to alter these distributions (Fig. 5, *panels to the right*) outside those regions below $T_{\min}$ and below the line with a slope of $\frac{1}{3}$ which extends from the point of initial density and temperature of the gas. This line corresponds to the path a uniform gas would take as a result of the imposition of a minimum temperature.

Recall from § 3.1 that individual structures in high-resolution simulations have, at early times, less shocked material in their cores than is produced at lower mass resolution. This difference is eliminated after the initial merging period on account of the introduction of new structures falling into the lower resolution cluster. These structures have material with low degrees of shocking. Compare the lower panels of Figure 1 with Figure 6 (*left panels*), which plots the ρ-T distribution for a cluster from a 32^3 and 64^3 simulation at late times (note that the figures have different scales). At early times, there is a population of less shocked gas in the high-resolution runs as described earlier. This leads to the spread in temperature at high densities. Although the distribution of substructures differs among the simulations of differing resolution, the presence of substructures at the termination of the simulations leads to a similar spread in temperatures, regardless of resolution. Taken as singular objects, the bulk properties of individual clusters do not vary substantially between simulations of differing resolutions. The degree of shocking, as parameterized by the entropy factor $\langle T\rho^{-\gamma}\rangle_M$ (a mass-weighted mean) is found to be essentially constant for the cluster simulated at either resolution. It is $(1.12 \pm 0.02) \times 10^{26}$ K cm^2 g$^{-2/3}$ for both the 32^3 and 64^3 simulations. With the imposition of a minimum temperature, the entropy is essentially unchanged at $(1.13 \pm 0.03) \times 10^{26}$ K cm^2 g$^{-2/3}$. The trend for the mean temperature of structures to increase with increasing resolution is maintained, with the gas temperature rising from $(2.9 \pm 0.1) \times 10^7$ K to $(3.2 \pm 0.1) \times 10^7$ K between the 32^3 and 64^3 simulations. This is understood to be a by-product of the deeper potential wells in the cores of structures as described earlier.

The density distribution confirms the similarity of the states of the gas in the simulations of differing resolution (Fig. 3, *solid line*). In the absence of a minimum temperature (Fig. 3, *left panels*), the gas density distribution varies marginally with resolution with a decrease in the amount of gas at a density of $\sim 10^{-29}$ g cm^{-3} compensated by an increase at the higher density of $\sim 10^{-27}$ g cm^{-3} as the spatial resolution is doubled. The addition of a minimum tem-

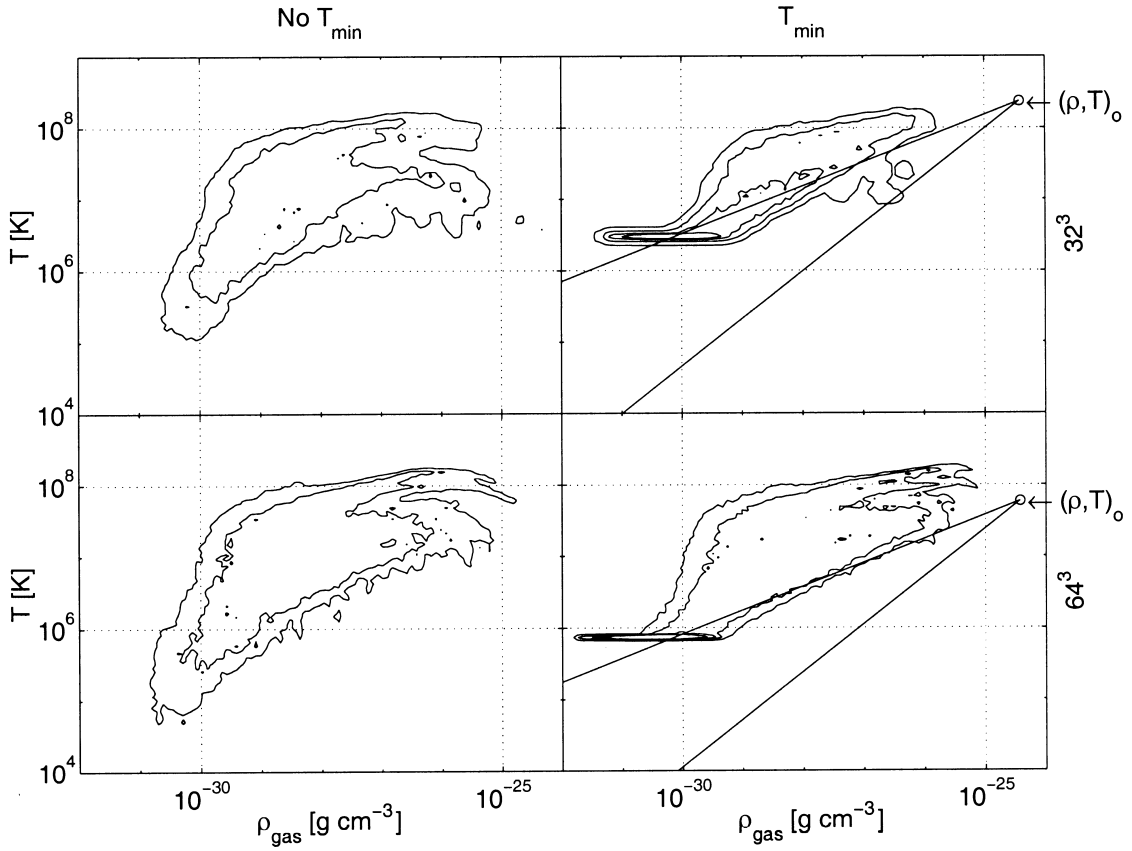

FIG. 5.—Temperature vs. gas density for all the gas at an expansion factor of $a = a_f$. The panels are as described in Fig. 4.

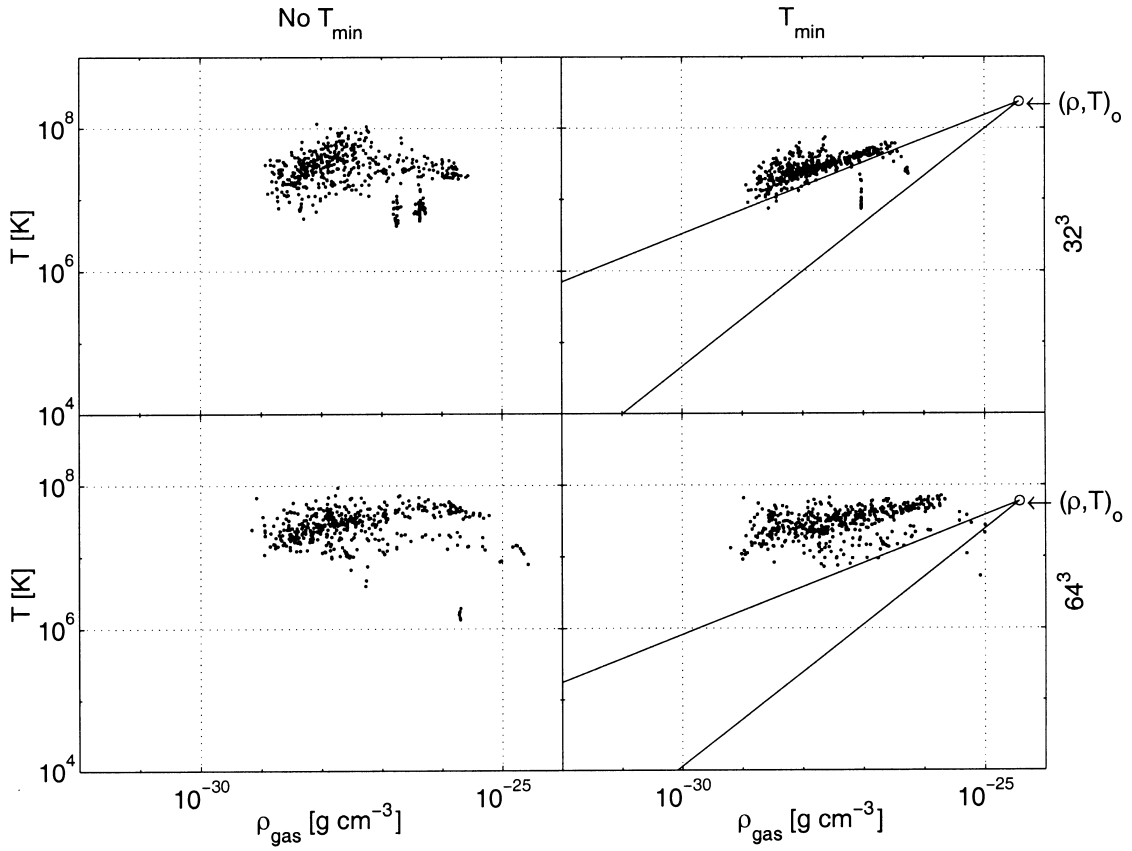

FIG. 6.—Temperature vs. gas density for the gas of a single cluster at an expansion factor $a = a_f$. The panels are as described in Fig. 4.

perature skews the distribution even more significantly to lower densities for the lower resolution simulation. The shift in the simulations without a minimum temperature can be explained as a result of the greater abundance of substructure in the dark matter distribution which locally compresses and heats the gas. The gas at the highest densities in the cores of structures ($\rho > 10^{-26}$ g cm^{-3}) is not significantly affected.

Finally, a useful diagnostic is the mean density profile (Fig. 2) of the clusters at the final epoch, $a = a_f$. It confirms that the presence of a minimum temperature does not change the morphology of the clusters. The mean profiles are calculated from a sample of clusters selected by their size, to ensure that the profiles are resolved. The inner cores are excluded from the calculation of the means, since they are not resolved.

3.3. *Baryon Fractions*

The simulations of OV97 display a marked tendency for the gas to become enriched in the cores of clusters, illustrated in Figure 9 of OV97. This is contrary to the results found by others (Evrard 1990; Thomas & Couchman 1992; Cen & Ostriker 1993; Kang et al. 1994a; Metzler & Evrard 1994; Pearce et al. 1994; Navarro et al. 1995; Anninos & Norman 1996; Lubin et al. 1996; Pildis et al. 1996). Indeed, it is most commonly found that the gas becomes more dispersed than the dark matter.

Depletion of gas in the densest regions is indicated by the simulations we performed. The baryon fraction parameter, Υ, which is the ratio of the baryon density to total mass density normalized by the global mean ratio, varies quite markedly with local density. In Figure 7, which is roughly comparable to Figure 9 of OV97, the mean normalized baryon fraction is plotted against the local overdensity of all matter, baryonic matter, and dark matter. The baryon fractions as well as the overdensities were measured in (400 kpc)^3 volumes evenly covering each simulation volume. This resolution is approximately half the numerical resolution of the 32^3 simulation. For Figure 9 of OV97, the ratio of the baryon particle density to the dark matter particle density is shown to rise well above unity in regions with high baryon overdensities. This effect is observed as well in our simulations (Fig. 7, *dot-dashed line*) but rolls over to less than unity as the baryon overdensity exceeds 10–200, independent of resolution. If the normalized baryon fraction is plotted against the true mass overdensity, (Fig. 7, *dashed line*), this initial increase in baryon concentration with increasing density is not observed at all. The baryon fraction decreases continuously with increasing local density. This suggests that the interpretation of Figure 9 of OV97 that the baryon fraction increases in regions of higher overdensity may be clouded by the selection effect of plotting it against local baryon overdensity. Essentially, their results only indicate that baryon fractions increase in regions of high *baryonic* overdensity.

In two dimensions, the only structures present are rods and sheets. Clusters are not simulated at all. Since our simulations demonstrate a depletion of baryons within the cores

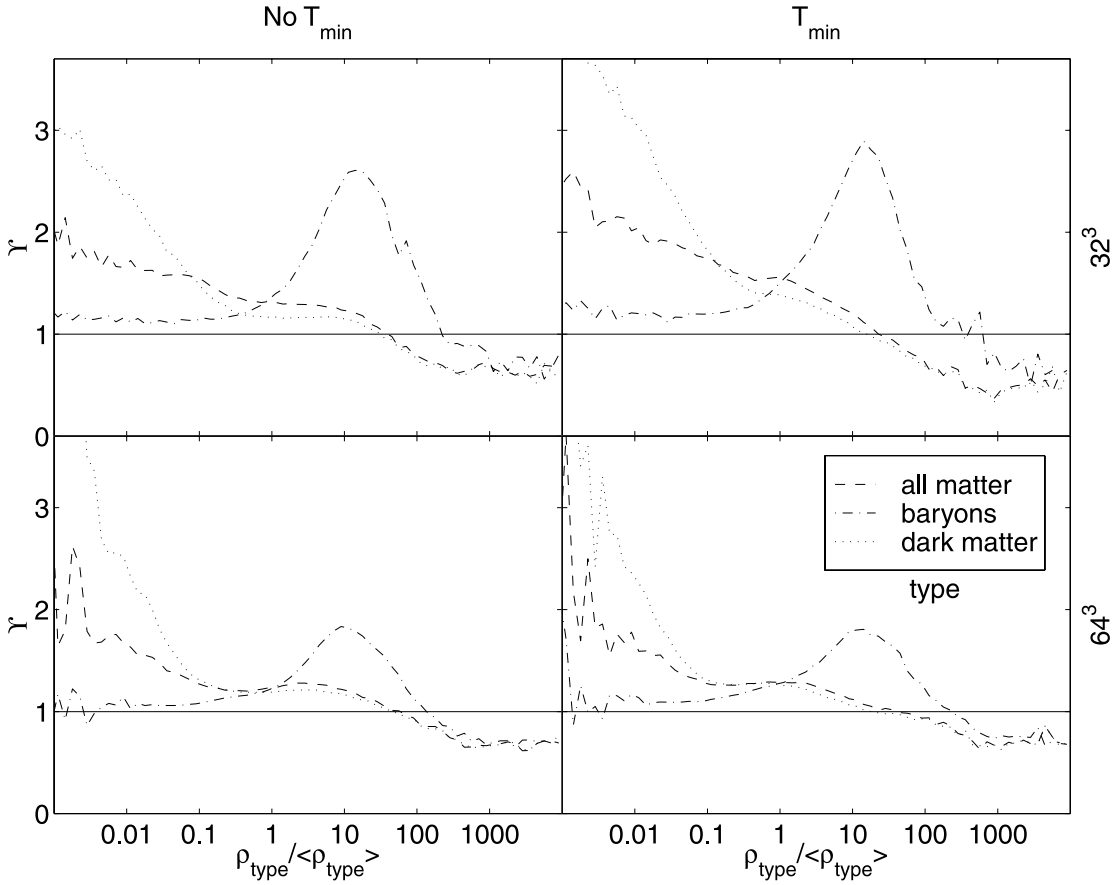

FIG. 7.—Normalized baryon fraction Υ vs. the local overdensity of all the matter (*dashed line*), the baryonic matter (*dot-dashed line*), and the dark matter (*dotted line*) in the presence or absence of a minimum temperature.

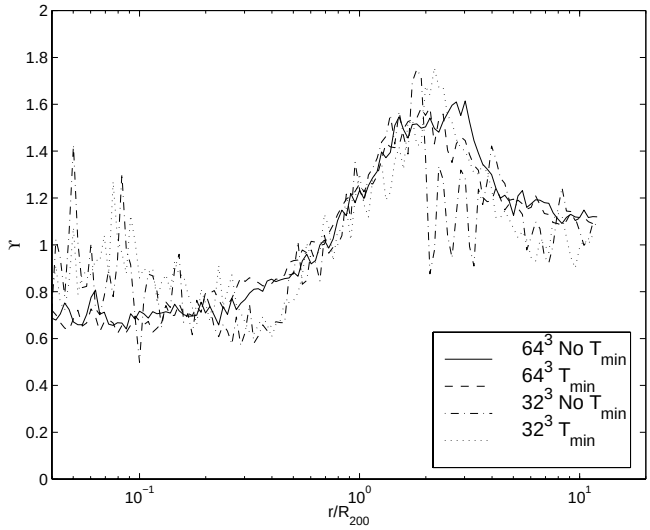

FIG. 8.—Radial profile of the mean baryon fraction parameter, Υ, for the clusters formed at different resolutions in the presence or absence of a minimum temperature.

of clusters and an enrichment within the other, less dense structures such as filaments and sheets, it may be possible to reconcile our results with those of OV97. Both sets of simulations indicate that the sheets and filaments are enhanced in baryonic material, relative to the total amount of matter. However, a crucial difference lies in the fact that these structures are enriched at the expense of the voids in the simulations of OV97, while for our simulations these structures are enriched at the expense of the clusters. They cannot, therefore, share similar causes.

Of importance in three-dimensional simulations of galaxy clusters is the baryon fraction profile. The normalized baryon fraction of clusters, derived from numerical simulations, is used to correct the baryon fraction measured from observations of galaxy clusters to produce a universal value (see Nevalainen, Markevitch, & Forman 1999, for example). The mean normalized baryon fraction profiles of the clusters in each simulation are plotted in Figure 8. They are for the same sample of clusters for which the mean density profiles have been calculated. It is clear from this figure that the presence of a minimum temperature has no effect on the baryon fraction distribution. It also shows clearly that resolution does have an effect in the cores.

4. DISCUSSION

It has been suggested (Owen & Villumsen 1997) that convergence with increasing mass resolution in numerical simulations of hierarchical structure formation requires the imposition of a minimum temperature in order for gas to be pressure-supported in structures with masses similar to the effective resolution of the simulation. Our results do not support this contention, either at early epochs after only a few mergers or at later epochs after a significant number of mergers have occurred and the minimum temperature has dropped well below the virial temperature of the typical structures. Our results indicate that the problem of the gas becoming overshocked in simulations in which the Jeans mass is not resolved is not as severe as suggested by OV97. The larger degree of shocking of the bulk of the gas noted by OV97 as resolution is lowered is not reproduced at any epoch of the simulations presented here. Consequently, the imposition of a minimum temperature is not necessary to achieve convergence.

We do observe a phenomenon that is similar to the decrease in shocking with increasing resolution as described in OV97. At an early epoch, isolated halos are shown to possess a large amount of substructure in their high-resolution simulations that is not present in their low-resolution counterparts. This substructure contains cool, dense, weakly shocked gas. However, the presence of this population of cool and dense gas in the high-resolution simulations is offset by an increase in the temperature of the halo gas surrounding these substructures. The net effect is not to lower the mean temperature of the halo but to marginally increase it (10% for each doubling in resolution) as well as to increase the entropy of the halo by an equivalent fraction. At a later epoch, after subsequent accumulation of material, the halos in the lower resolution simulations develop a comparable population of cooler, unshocked gas within substructure.

Further attempts were made to reproduce the results of OV97 by modifying our code. Since it was believed that the gravity calculations for the simulations of OV97 were done using a particle-mesh method, we disabled the particle-particle contributions of the gravitational force as well as the refinements in the HYDRA code. The minimum temperature that scales with the expansion factor that is used in these simulations was replaced with a constant minimum temperature of the form used in OV97. Both of these changes were unsuccessful in reproducing the results of OV97.

The results of imposing a minimum temperature sufficient to pressure-support the resolution-limited gas structures were examined for adverse effects. At the final epoch, the gas density profiles of the clusters were not altered. The degree of shocking increased by less than 5%. This increase may be attributed primarily to an increase in temperature and decrease in density of the gas lying near the cores of structures. The bulk of the gas, which lies in the halo, was unaffected.

The concentration of baryonic material in the cores of structures reported by OV97 is also not observed. Instead, an antibias is found, in accordance with the substantial majority of numerical simulations reported in the literature as noted previously. Pearce et al. (1994) explain the phenomenon as a result of the merging process of gas–dark matter halo systems in which gas is shocked, permanently removing the energy from the dark matter component. For the gas to be more biased in clusters, without an energy-loss mechanism operating such as cooling, the gas must transfer energy to the dark matter component. We note that the results of OV97 may be influenced by a selection effect due to their identification of overdense regions by regions overdense in baryonic material.

It is unclear what causes the differences between our results and those of OV97. The most striking remaining difference between our investigations and those of OV97, which we have not explored, is the difference in dimensionality of the numerical simulations. OV97 used two-dimensional simulations, while ours were three-dimensional. Structures in two dimensions are rods, which have essentially the same cross sections per unit mass as spheres, but one less degree of freedom in which to avoid collisions. This may strongly affect the efficiency of shock heating, with more head-on collisions per merging event

leading to more violently shocked gas. However, naive interpretation of this observation would suggest that the gas halos should be more extended, and more antibiased relative to the dark matter, contrary to the results of OV97.

We conclude that resolution of the Jeans mass of the smallest structures is consequently not important in studies of the gas in structures after merging has occurred. It may be important for the first objects formed, but for any study other than the statistics of position and number, these first objects should be ignored, since they are, by definition, poorly resolved. Clearly, this result may not hold for simulations in which there is cooling and/or star formation feedback, but these will have an effect only in the densest parts of the clusters, and should not affect global properties.

We thank Rob Thacker for helpful discussions as well as the anonymous referee for useful comments. H. M. P. C. acknowledges the support of NSERC.

REFERENCES

Anninos, P., & Norman, M. L. 1996, ApJ, 459, 12
Bryan, G. L., Cen, R., Norman, M. L., Ostriker, J. P., & Stone, J. M. 1994, ApJ, 428, 405
Cen, R. 1992, ApJS, 78, 341
Cen, R., Miralda-Escudé, J., Ostriker, J. P., & Rauch, M. 1994, ApJ, 437, L9
Cen, R., & Ostriker, J. P. 1993, ApJ, 417, 404
Couchman, H. M. P., Thomas, P. A., & Pearce, F. R. 1995, ApJ, 452, 797
Davis, M., Efstathiou, G., Frenk, C. S., & White, S. D. M. 1992, Nature, 356, 489
Evrard, A. E. 1990, ApJ, 363, 349
Evrard, A. E., Metzler, C. A., & Navarro, J. F. 1996, ApJ, 469, 494
Frenk, C. S., et al. 1999, ApJ, 525, 554
Gnedin, N. Y. 1995, ApJS, 97, 231
Hernquist, L., & Katz, N. 1989, ApJS, 70, 419
Kang, H., Cen, R., Ostriker, J. P., & Ryu, D. 1994a, ApJ, 428, 1
Kang, H., Ostriker, J. P., Cen, R., Ryu, D., Hernquist, L., Evrard, A. E., Bryan, G. L., & Norman, M. L. 1994b, ApJ, 430, 83
Katz, N. 1992, ApJ, 391, 502
Katz, N., & Gunn, J. E. 1991, ApJ, 377, 365
Lubin, L. M., Cen, R., Bahcall, N. A., & Ostriker, J. P. 1996, ApJ, 460, 10
Metzler, C. A., & Evrard, A. E. 1994, ApJ, 437, 564
Moore, B., Governato, F., Quinn, T., Stadel, J., & Lake, G. 1998, ApJ, 499, L5
Navarro, J. F., Frenk, C. S., & White, S. D. M. 1995, MNRAS, 275, 720
Navarro, J. F., & White, S. D. M. 1993, MNRAS, 265, 271
Nevalainen, J., Markevitch, M., & Forman, W. 1999, ApJ, 526, 1
Owen, J. M., & Villumsen, J. V. 1996, preprint (astro-ph/9603156)
———. 1997, ApJ, 481, 1 (OV97)
Peacock, J. A. 1999, Cosmological Physics (Cambridge: Cambridge Univ. Press)
Pearce, F. R., Thomas, P. A., & Couchman, H. M. P. 1994, MNRAS, 268, 953
Pildis, R. A., Evrard, A. E., & Bergman, J. N. 1996, AJ, 112, 378
Ryu, D., Ostriker, J. P., Kang, H., & Cen, R. 1993, ApJ, 414, 1
Steinmetz, M. 1996, MNRAS, 278, 1005
Steinmetz, M., & Müller, E. 1993, A&A, 268, 391
Thomas, P. A., & Couchman, H. M. P. 1992, MNRAS, 257, 11
Tittley, E. R., & Couchman, H. M. P. 1999, preprint (astro-ph/9911365)
Zeldovich, Ya. B. 1970, A&A, 5, 84